Hindawi
Advances in Meteorology
Volume 2021, Article ID 2047609, 13 pages
https://doi.org/10.1155/2021/2047609

Research Article

Convective Cold Pool Associated with Offshore Propagation of Convection System over the East Coast of Southern Sumatra, Indonesia

Erma Yulihastin,[1] **Ibnu Fathrio**,[1] **Trismidianto**,[1] **Fadli Nauval**,[1] **Elfira Saufina**,[1] **Wendi Harjupa**,[1] **Didi Satiadi**,[1] **and Danang Eko Nuryanto**[2]

[1]*Research Center of Atmospheric Science and Technology, Research Organization of Aeronautics and Space, National Research and Innovation Agency, Bandung, West Java 40173, Indonesia*
[2]*Research and Development Center, Indonesian Agency for Meteorology Climatology and Geophysics, Jakarta Pusat 10720, Indonesia*

Correspondence should be addressed to Erma Yulihastin; erma.yulihastin@lapan.go.id

Received 20 April 2021; Revised 22 July 2021; Accepted 26 August 2021; Published 28 September 2021

Academic Editor: Mario M. Miglietta

The cold pool outflow has been previously shown to be generated by decaying Mesoscale Convective Complexes (MCCs) in the Maritime Continent. The cold pool also has a main role in the development processes of oceanic convective systems inducing heavy rainfall. This study investigated a cold pool event (January 1-2, 2021) related to a heavy rainfall system over the coastal region of Lampung, Southern Sumatra, within a high-resolution model simulation using a regional numerical weather prediction of the Weather Research and Forecasting (WRF) with convection permitting of 1 km spatial resolution, which was validated by satellite and radar data observations. It is important to note that the intensity, duration, timing, and structure of heavy rainfall simulated were in good agreement with satellite-observed rainfall. The results also showed that a cold pool (CP) plays an important role in inducing Mesoscale Convective Complex (MCC) and was responsible for the development of an offshore propagation of land-based convective systems due to the late afternoon rainfall over inland. This study also suggests that the propagation speed of the CP 8.8 $m{\cdot}s^{-1}$ occurring over the seaside of the coastal region, the so-called CP-coastal, is a plausible mechanism for the speed of the offshore-propagating convection, which is dependent on both the background prevailing wind and outflow. These conditions help to maintain the near-surface low temperatures and inhibit cold pool dissipation, which has implications for the development of consecutive convection.

1. Introduction

Convective cold pools are near-surface regions of downdraft areas that are spread out horizontally along the convective line underneath precipitating clouds [1–4]. Two plausible mechanisms of the cold pool (CP) that generated new convective cells have been proposed by the previous studies [5, 6]: (1) lifting of near-surface environmental air by dense and cold air might produce new convection cells along the convective line; (2) developing of convective available potential energy (CAPE) and decreasing of convective inhibition (CIN) by both sensible and latent heat fluxes might change the surface into cold pool air [5, 7, 8]. Both previous observational and numerical studies suggest that CP plays an important role to develop new convective cells as well as maintain the formation of a long-lasting mesoscale convective system (MCS) under the squall-line mechanism [5, 9–14]. On the other hand, for the coastal region, the front sea breeze systems could produce cold pools associated with the previous precipitation process. The sea breeze system is also controlled by the spatial distribution of local sea surface temperature under the coastal convergence line mechanism [15, 16] which may have high variation due to the coastal dynamics [17].

Herein, as the CP is a key feature to organize deep convective clouds over midlatitude regions, the existence of CP over the lesser latitude, that is, the Maritime Continent, still had been questionable and not yet understood. However, limited studies have mentioned the CP as a responsible mechanism to develop propagating convective systems related to diurnal rainfall propagation speed over the Maritime Continent [18–24]. On the other hand, propagating convective systems over coastal regions is the main characteristic that may produce enhanced rainfall related to extreme events [24–26].

In this study, we considered a heavy rainfall event during January 1-2, 2021, over Lampung province, South Sumatra, which triggered severe floods in the following days. The flood hits several parts of Lampung leading to loss and damage of hundreds of houses and also causing 250 families to be isolated, on January 5, 2021 [27]. It should be noted that the Lampung province is bordered by Java Sea and Sunda Strait and is relatively near Jakarta Bay. For several Jakarta floods, South Sumatra has an important role in developing offshore propagation over Java Sea which may interact with northerly wind-produced heavy rainfall associated with early morning precipitation over the north coast of West Java [24], particularly Jakarta City, the capital of Indonesia.

This study used a numerical simulation to investigate a CP event related to heavy rainfall that hits Lampung, South Sumatra, on January 1-2, 2021. We used Weather Research and Forecasting (WRF) model [28], with initial and boundary conditions derived from the National Center for Environmental Prediction Final Analysis (NCEP-FNL) whose spatial and temporal resolution are 0.25° and 6 hours, respectively, to conduct a high-resolution simulation with convection permitting of 1 km resolution. We further analysed the simulation results by comparison with the detailed characteristics of the convective clouds over Lampung as revealed by satellite imageries as well as radar observation during the heavy rainfall period. In the next sections, we discuss the data used in this study, model setup and configuration, and results of both the observation and simulation.

2. Data and Methods

In this case study of heavy rainfall, we are concerned with investigating the role of a cold pool in developing thunderstorms associated with the MCC. We then divided the methodology into two stages. Firstly, we explore synoptic analysis to explain the background condition related to the heavy rainfall event. Secondly, in order to identify the cold pool and the MCC, we used both observed and simulated data. We examined satellite and radar data observation as well to confirm the model data simulation.

When a thunderstorm develops, clouds may be fully formed and start producing precipitation. This condition could create a cold pool in the lower level due to the downward advection of cold air. In order to identify a cold pool, we examined 2 criteria: (1) Potential temperature decreases over near surface [5]. In this case, we used equivalent potential temperature <340 K over near surface (<1 km) as a cold pool. (2) The existence of cold pool is also characterised by divergent outflow from the cloud so that we used cloud and wind surface data as the data supported. These variables will be carried out from the model simulation.

Furtherly, to confirm the convective activity during the study period, radar reflectivity records obtained from Meteorology, Climatology, and Geophysics Agency (BMKG) radar was used to observe the spatial distribution of precipitation. In this case, to capture the wider regions due to global scale, we also used precipitation data obtained from the Global Satellite Mapping of Precipitation (GSMaP) with 0.1° spatial resolution [29]. Other primary data to confirm the convective clouds are Black Body Temperature (TBB) data retrieved from band 13 of Himawari satellite observation [30] which has a spatial and temporal resolution of 4 km and 10 minutes, respectively.

In addition, to determine convective cloud systems, we plotted spatial analysis of TBB data in a time evolution during the event periods. The duration of deep convective cores is identified by low TBB values (<221 K) [31], whereas the minimum threshold for convective cloud top temperature is 241 K following the method to obtain Mesoscale Convective Complex (MCC) from satellite data [32]. Identification of CP needs to be addressed to the cloud-induced surface flows which could be calculated by wind vector anomalies following [20] from the cross-calibrated multiple satellite (CCMP) reanalysis datasets [33, 34], covering global oceans with 6-hourly temporal resolution and 25 km spatial resolution.

In this study, we identified a cold pool by using simulation of Weather Research Prediction (WRF) models of WRF.4.2 [28] designed in one-way three nested domains with 9 km (D01), 3 km (D02), and 1 km (D03) spatial resolution and 33 vertical grids (Figure 1). Betts Miller Janjić was used as a cumulus scheme on the first and second domain, while a no-cumulus scheme was used for the third domain. Details of the scheme used in this study following Fonseca et al. [35] produced the best qualitatively agreement in simulating diurnal precipitation intensity over MC, as shown in Table 1.

Initial and boundary conditions were obtained from the National Center for Environmental Prediction/National Global Data Analysis System (NCEP GDAS)/FNL 0.25 Degree Global Tropospheric Analyses and Forecast Grids [36]. The FNL was chosen as a model input since the NCEP global prediction skills have increased for the two decades recently (i.e., Kalnay, 1996) [37], although the FNL data over the MC region still remain lower quality compared to observational data. However, in this case, we have assumed that NCEP-FNL data are good enough to support our present research purpose.

2.1. Model Setup and Experimental Design. In the present work, simulation was integrated for 72 hours, starting from December 31, 2020, 12:00 UTC (19:00 LST) until January 03, 2021, 00:00 UTC (07:00 LST), with the first 12 hours considered as spin-up time. In previous work, one-way nesting

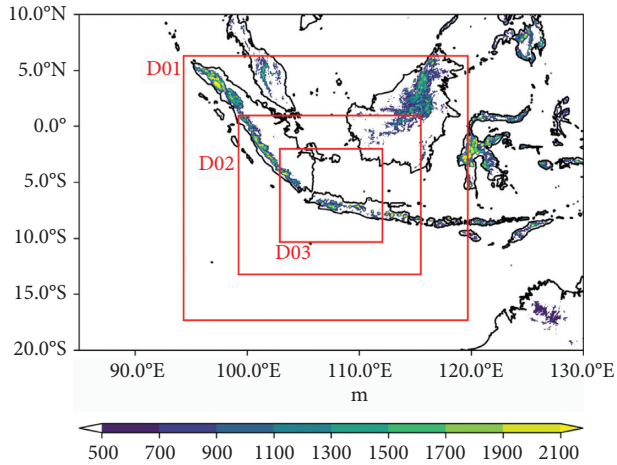

Figure 1: Simulation domain of WRF model. The red boxes represent domains 1, 2, and 3 for 1, 3, and 9 km resolution, respectively. Colour shaded shows height terrain over islands.

for 3-domain simulation of WRF model could produce a good agreement to capture rainfall intensity and offshore-propagating convective system over Papua New Guinea and vicinity, the eastern part of Maritime Continent [38]. For qualitative as well as quantitative validations of rainfall intensity, timing, duration, and location, we used data observations from the BMKG station, radar, and GSMaP satellite. On the other hand, it is also important to notice that, in the present work, we were mainly concerned with simulating CP as a dynamical process responsible for the mechanism of heavy rainfall events related to the Lampung flood on January 6, 2021. In this case, the model parameters (equivalent potential temperature, cloud water content, and wind) should be selected to simulate realistic atmospheric flows representing a CP phenomenon in a high temporal resolution (10 minutes).

3. Results and Discussion

3.1. Synoptic Condition. Synoptic weather conditions from December 30 to January 2, 2020, were examined using both the satellite and NCEP-FNL data. Figure 2(a) shows that convective activities were predominant over southwest Indonesia from December 30 to 31, as indicated by the distribution of low Black Body Temperature (TBB) concentrated over the Java Ocean and the southwest Indian Ocean off the south of Sumatra. On the other hand, combinations between anticyclonic vortices over the South China Sea and North Sumatra develop convergence zones over most of Sumatra in this period (Figure 2(b)).

It should be noticed that the Borneo vortex which started developing from January 1, 2021, enhanced convective activity elongated over the east coast of Sumatra but seems not to extend to the south of Sumatra. However, strong westerly moisture transport intrusion occurred over southern Sumatra coming from the northern monsoon from the South China Sea. The combination of Borneo vortex development and southeast cyclonic vortex existence over north Australia causes strengthening of predominantly north-westerly moisture transport and develops convergence system over the south of Sumatra.

Although the effects of the predominant north-westerly moisture transport might have contributed to large amounts of rainfall over the south of Sumatra, it seemed to be concentrated to limited areas due to less convective activity in a daily average of January 1-2, 2021 (Figure 2(a)). To understand the causes of this condition, we further analysed the diurnal variation of convective activity and rainfall on January 1–2 over the study area from satellite data of both GSMaP and Himawari (Figure 3).

3.2. Heavy Rainfall Observed. Heavy rainfall observed by GSMaP satellite data revealed a large quantity of rainfall accumulation occurring on January 1 over the entire region in the south of Sumatra and the maximum intensity (>110 mm·d^{-1}) concentrated over the east coast of Lampung and ocean around the coastal region (Figure 3(a)). The timing of heavy rainfall starts from January 1 afternoon (18:00 LST) over inland and persists to early morning the following day (02:00 LST) (Figure 3(b)). In this case, land-based convective systems seem to have an offshore propagation due to mesoscale convective systems with the maximum convection remaining occurring over inland (Figure 3(c)). This discrepancy of location between maximum rainfall and maximum convection indicated that the dynamical process that caused offshore propagation of diurnal rainfall might have been related to the "self-replicating" mechanism into an internal deep cloud system near the coastal region, as suggested by [18].

This mechanism needs to be confirmed by further investigation of time evolution of the convective system (Figure 4(c)–4(e)). It is found that the initial convection occurred over the west coast of southern Sumatra in a small area starting from January 1 at 13:00 LST (4.8°N, 104°E) (see Figures 4(a) and 4(d)). It is important to note that the convective system developed rapidly as an MCC at afternoon time (19:00 LST) influenced by a large convergence system between north-westerly from Java Sea and south-westerly from the Indian Ocean (Figures 4(b) and 4(f)). A single developed to multiple convection cells of MCC appeared clearly in (Figures 4(e) and 4(f)), which need to be explored in a detail hourly time evolution in further analysis (Figure 5).

3.3. Cold Pool-Induced Mesoscale Convective Complex. It was noticed that the life cycle of the MCC occurred more than 6 hours on January 1 (19:00–02:00 LST), confirmed by both rainfall radar and cloud satellite observation (Figure 5). This MCC starts with a contiguous cold cloud shield at about 24.000 km^2 and grows promptly to ~55.000 km^2 at 20:00 LST (Figure 5(b)). The MCC is identified by a contiguous cold cloud shield (TBB ≤ 241 K) more than 50.000 km^2 following [31]. More interestingly, the MCC developed from single (19:00 LST) to three convective cells (21:00 LST) with the new convective cells propagating out of phase to offshore propagation direction (Figure 5(b)). This developing process of the new convective cells in MCS consistent with previous

Table 1: Model configuration of WRF for simulating precipitation over the Maritime Continent with horizontal resolutions: 9 km (D01), 3 km (D02), and 1 km (D03).

Horizontal resolution	9 km	3 km	1 km
Number of horizontal grids	300 × 300	400 × 400	634 × 532
Number of vertical grids	33	33	33
Cumulus	Betts Miller Janjić	Betts Miller Janjić	—
Microphysics	WSM-3	WSM-3	WSM-3
Long-wave/short-wave radiation	RRTM/Dhudia	RRTM/Dhudia	RRTM/Dhudia
Boundary layer	Yonsei University	Yonsei University	Yonsei University
Surface layer	Revised MM5 Monin–Obukhov	Revised MM5 Monin–Obukhov	Revised MM5 Monin–Obukhov
Land surface	NOAH	NOAH	NOAH

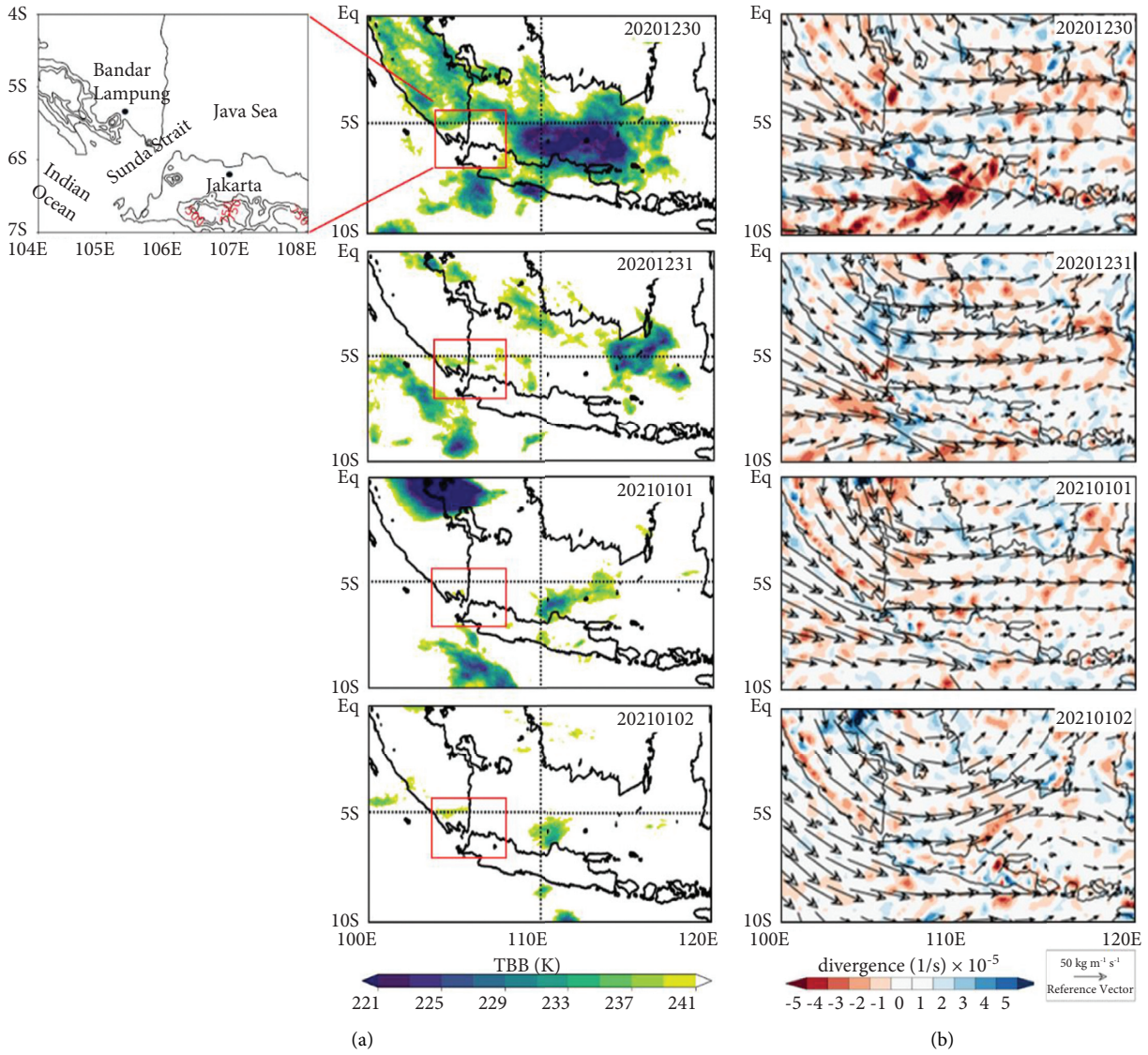

Figure 2: Time evolution from December 30, 2020, to January 2, 2021, for (a) spatial distribution of daily averaged TBB derived from IR1 Himawari satellite imageries; (b) daily averaged vertical integrated of moisture transport (vector) and divergence (shaded) plotted from the NCEP-FNL data, corresponding to the TBB map of the left panels. The area of interest is indicated by a red-square box.

studies explained a back-building mechanism [39–41] which mainly produced extreme rainfall [39].

Figure 5(b) shows that the MCC developed rapidly and largely and also propagated offshore and extended over the entire region of southern Sumatra and Java Ocean off the east coast of Sumatra. It was also clearly exhibited that, during the early morning, new convective cells occurred over the ocean (Figures 5(a) and 5(b)). In this case, during

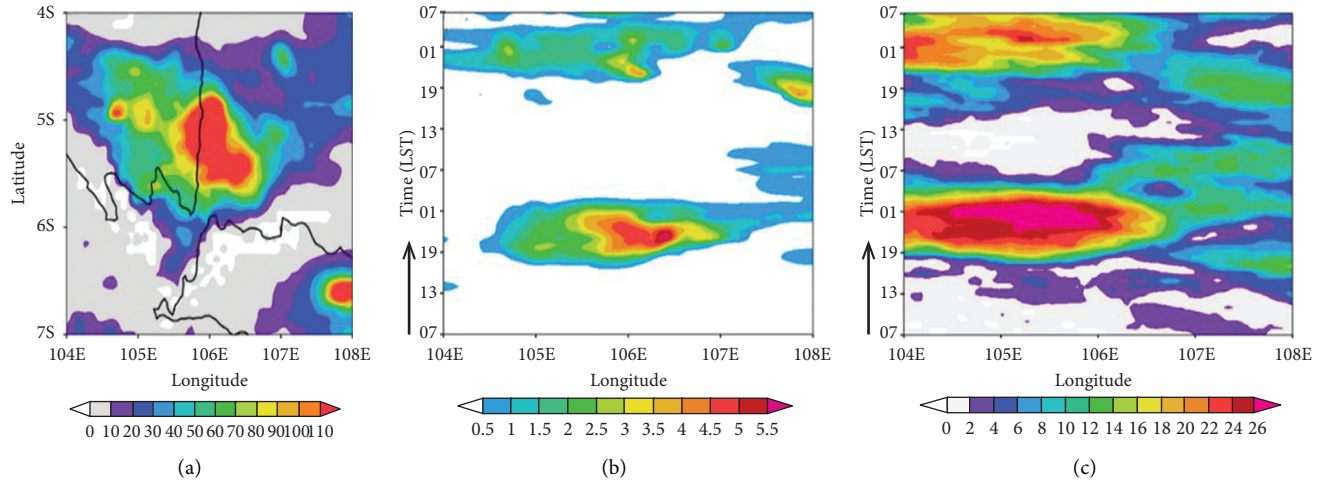

FIGURE 3: (a) Daily accumulation of rainfall from GSMaP on January 1-2, 2021; (b) Hovmöller of time-longitude cross section of rainfall from GSMaP, averaged for 5-6°N; (c) same as (b), but for convective index from Himawari satellite.

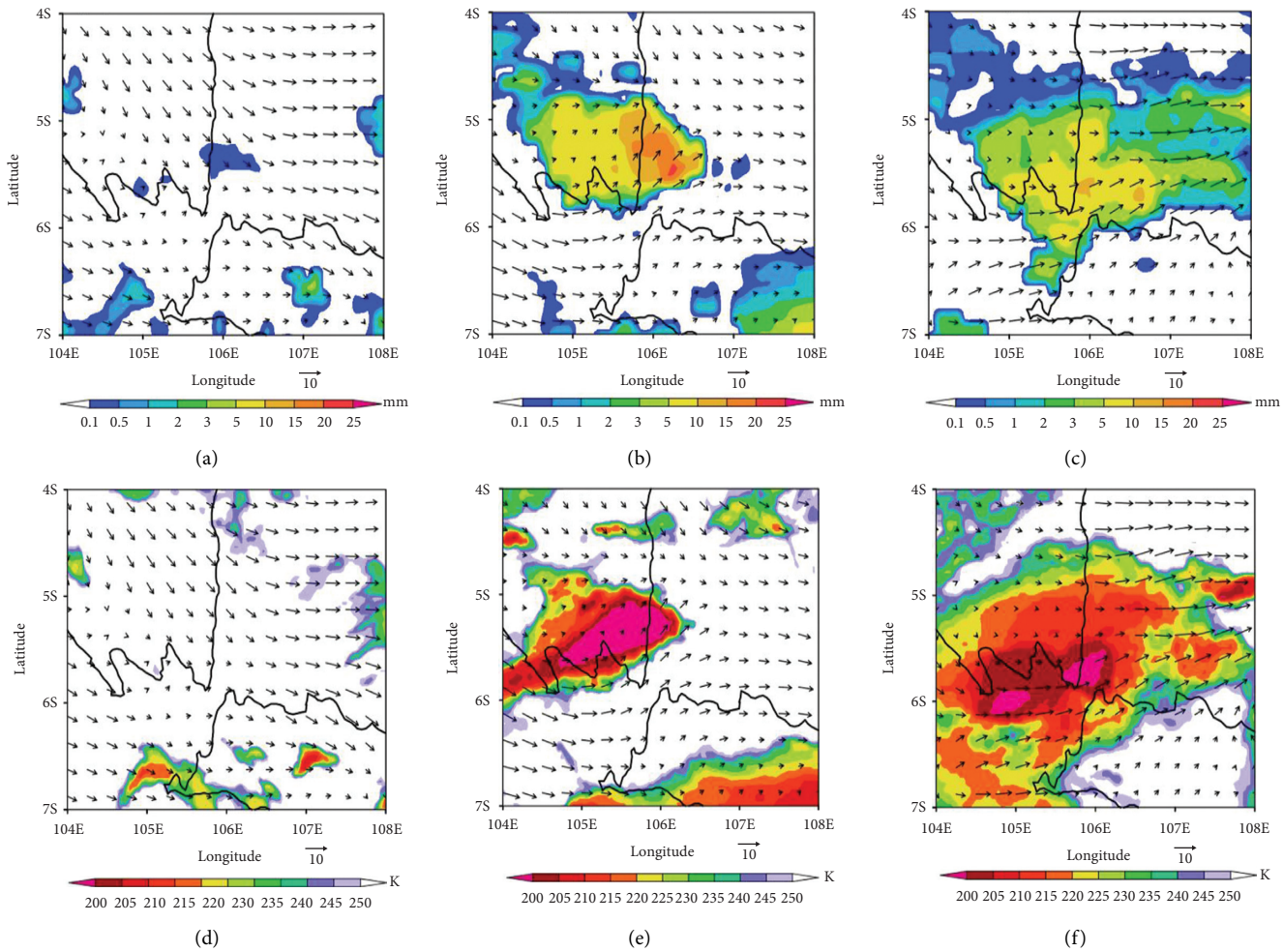

FIGURE 4: (a–c) evolution of observed rainfall and surface wind derived from GSMaP and CCMP data, respectively, during January 1-2, 2021, for (a) 13:00 LST; (b) 19:00 LST; (c) 01:00 LST. (d–f) same as the upper panel, but for temperature black body (TBB) of cloud from Himawari satellite.

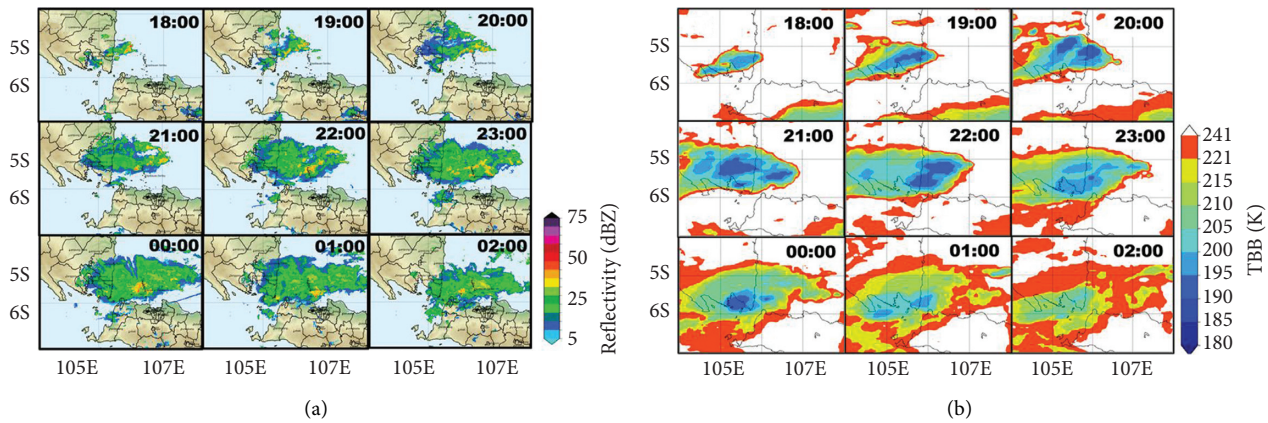

Figure 5: Hourly evolution of January 1-2, 2021, from 18:00 to 02:00 LST for (a) rainfall observed by BMKG radar and (b) mesoscale convective complex from Himawari satellite. The colour gradation from yellow to blue indicates interior cold cloud with TBB ≤ 221 K and brown colour indicates cloud shield with 221 K ≤ TBB ≤ 241 K.

the dissipation process, the MCC also produced other cells of the convection system in the early morning on the following day (01:00-02:00 LST) (Figure 5(b)). The MCC has a long-lasting existence from initiation to dissipation (>6 h) which was closely related to the development of the mesoscale convective system (MCS) that lasted for more than 10 h [40, 41]. It is also interesting to note that oceanic systems have a longer duration (~14 h) and hit a slightly smaller region compared to continental systems [42].

Closer inspection of the heavy rainfall evolution based on GSMaP satellite data revealed that the initial stage of deep convective cloud starts from January 1 at 18:00 LST and further develops to MCC and expands in a wide region over inland as well as coastal region (Figure 6(a)). It also noticed that the core of MCC seems to be migrating offshore at 20:00 LST during the mature stage of MCC. The decaying process of MCC at 21:00 LST was continued until 23:00 LST by developing new convections over the coastline as well as ocean regime. This mechanism related to the development of new convective clouds over the Maritime Continent is consistent with a previous study [21] that stated that MCC may induce cold pool-like environments by the so-called sprinkler effects. The hourly evolution of MCC which is represented by the onset of heavy rainfall observed seems to be qualitatively well simulated by the model (Figure 6(b)). The timing of the initial rainfall system at 18:00 LST and the maximum rainfall at 21:00 LST over the seaside of the coastal region could be produced well by the model. Moreover, the model is also able to simulate offshore propagation of rainfall system (Figure 6(b)).

It is important to note that the maximum intensity, duration, and structure of a heavy rainfall event on January 1 (18:00–02:00 LST) were qualitatively well simulated by model results (Figure 6(b)). The initial convection which began from January 1 at 10:00 LST over inland (5°N; 104.8°E) by a single-small rainfall cell also could be produced well by the model (figure not shown). The model results also depict several rainfall cells elongated as a rainband from inland to the coastal region at 18:00 LST. The rainfall system represents a land-based convective system that propagates offshore, influenced by north-westerly monsoon flow as a predominant background wind.

Moreover, to test quantitative agreement between simulated and observed rainfall results in timing, maximum intensity, and location, we further used station and satellite data observation. At first, the simulated data that needs to be confirmed with the terrestrial-based data was revealed from BMKG station over three locations around Lampung province, that is, Rajabasa, Sukabumi, and Tanjung Senang (Figure 7(a)), where the detailed locations on the map are described in Figure 7(b). The daily accumulation of rainfall from December 25 to January 2, 2021, shows that modulation of heavy rainfall occurred on January 1, 2021, with the highest value (~40 mm) occurring in Tanjung Senang (Figure 7(a)). Secondly, the statistical analysis was applied for satellite data by using composite and area-averaged methods during January 1-2, 2021, over landside and seaside of the coastal region, respectively (Figure 7(c)), which is related to the box areas (Figure 7(d)).

For the timing of maximum rainfall, the model captured it in a concurring time (22:00 LST) between landside and seaside regions. This maximum rainfall over the landside region captured by the model has been delayed 2 hours later compared to satellite (Figure 7(c)) and radar (Figure 7(e)) data (20:00 LST). This discrepancy is more sophisticated than previous studies that found 3–15 different hours of maximum timing in diurnal rainfall over the coastal region of Sumatra, as interpreted in Figure 5 [43]. It is important to note in previous studies that although spatial model resolution improved, the model seems still incapable to simulate principal processes concerning rainfall due to land-based as well as oceanic-based convective systems.

It is also interesting to note that the vertical structure of MCC was well-observed by the radar data with deep convective clouds reaching ~11 km height (Figure 7(e)). The existence of 3 convective cells exhibited over low levels (<4 km) with the contour was filled by grey colour. This quasistationary convection system during 19:00–20:00 LST, the so-called back-building mechanism, corresponds to previous evidence captured by the Himawari satellite

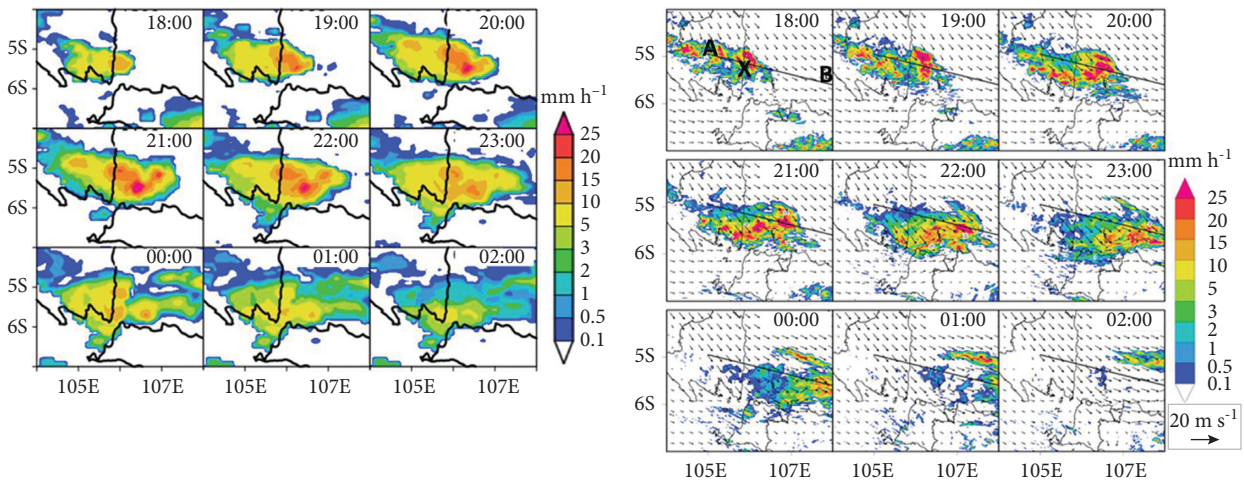

Figure 6: Same as Figure 5, but for (a) observed hourly rainfall from GSMaP satellite data; (b) simulated hourly rainfall and wind vector (925 mb) from domain 3 of WRF model simulation. A-B transect delineated through coastline (X) (105.85°E, 5.15°S) used for further analysis in Figures 8 and 9.

(Figure 5(b)). However, the role of cold pools in producing new convective cells under the back-building mechanism needs to be further investigated by the model simulation.

For the maximum intensity issue, the rainfall observed by the GSMaP satellite occurred at 23:00 and 20:00 LST for landside and seaside, respectively. In this case, the simulated results also consistently show overestimation with rough calculation around 2-3 mm compare to rainfall maximum observed. These values are also relatively small compared to the previous study that simulated heavy rainfall threshold which estimated ~20–40 mm compared to observed rainfall (2–4 mm) over West Java, Indonesia [44]. In this case, although the model lacks the capability to capture the semidiurnal signal of diurnal rainfall over the landside (Land1), it is still good agreement to simulate the development of rainfall system from initial to decaying stage, which is strongly related to reinforcement of new convective cells (Figure 7(c)). In order to understand this development of the convective cells, we need to further investigate it by simulating model resemblances.

3.4. Role of Cold Pool on Propagation of Convection System. To understand the dynamical processes of this offshore rainfall propagation, we further explore the vertical-longitudinal distributions of vertical wind, water vapor mixing ratio, and equivalent potential temperature (Figure 8). The intense rainfall center extended south-eastward from inland to the east coastline of Lampung, southern Sumatra, which is generated by several convective clouds at 18:00 LST. The decaying cloud over inland (A, 105°E) induced a cold pool (CP), the so-called "CP-inland," over around 0.5 km and created a new convective cloud over 50 km distance to the coastline (X) at 19:00 LST. At the same time, another cold pool also developed over the coastline, that so-called "CP-coastline" from the decaying convective cloud. Additionally, CP-inland seems to have dissipated in the following time (20:00 LST) due to strong south-eastward flow and lack of environmental support related to minimum near-surface moisture. On the other hand, a decaying convective cloud over the seaside at around 10 km from the coastline (106°E) created a cold pool and generated a new convective cloud in the leading edge. However, we need to investigate the decaying process of CP-inland from 19:00 to 20:00 LST in more detail in the following analysis in Figure 9.

From Figures 8 and 9, we could also remark that the evolution of convective cells by the CP is clear to follow. Deep convection appeared at 18:00 LST over inland (CP-inland) and coastline (CP-coastline). The CP-inland still existed from 19:00 LST to 19:30 LST and then dissipated with the outflow of the CP which tends to strengthen the CP-coastline, which is produced from another decaying process of convective cloud over the coastline at 19:00 LST. The CP-coastline was triggered resembling a "back-building" mechanism in a mesoscale convective system (MCS), particularly from 19:30 to 19:40 LST (Figure 9). It was clearly shown that the new convection cell produced landward from the offshore convection system which was relatively stationary over C location (154 km from the coastal line). This new convection then merged with offshore convection and propagated over almost 100 km offshore at 21:40 LST (Figure 9).

At 22:00 LST, the CP-coastal continued to propagate offshore and seemed to have induced deep convection leeward over the seaside of the coastal region (Figure 8). At the same time, another deep convection windward over the leading edge of CP was also developed resembling a "back-building" mechanism. The offshore propagation of several

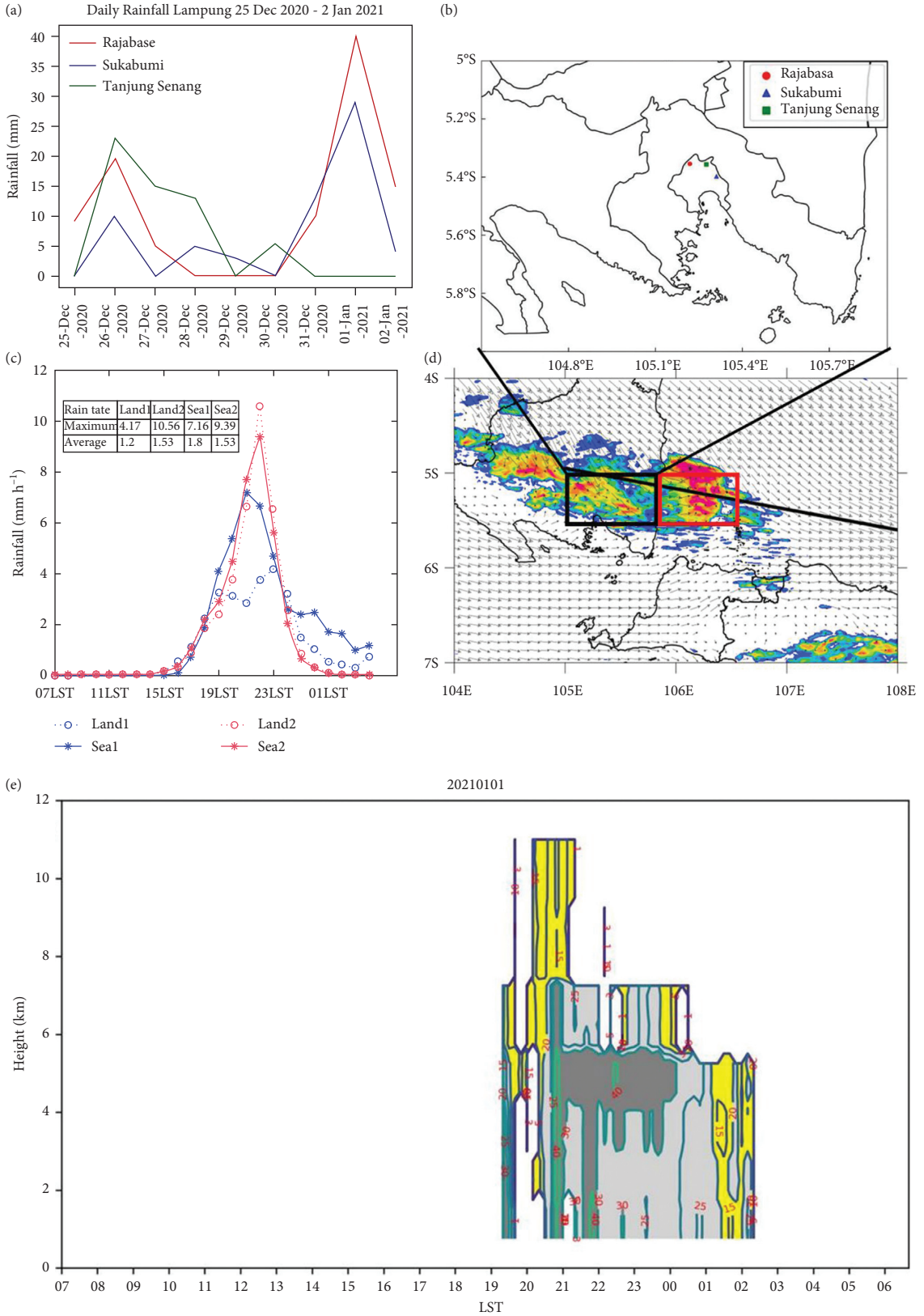

FIGURE 7: (a) Time series of daily accumulation of rainfall from BMKG station during December 30, 2020–January 2, 2021. (b) A map of the 3 station data locations. (c) Comparison of simulated diurnal rainfall (mm h^{-1}) at D03 (1 km) resolution with GSMaP satellite. Rainfall over seaside (landside) from GSMaP (WRF) is denoted as Sea1 (Sea2) and Land1 (Land2), respectively. (d) The landside and seaside area denoted for area averaged over 105–105.8°E 5.5–5°S (black box) and 105.8–106.5°E; 5.5–5°S (red box) of the eastern coastal region of South Sumatra. The average diurnal cycle is composited from January 1 to January 2, 2021. (e) Diurnal rainfall observed by radar reflectivity (dBZ) height-time cross section of radar reflectivity (dBZ) over X (105.85°E, 5.15°S as a center area of Lampung at January 1, 2021.

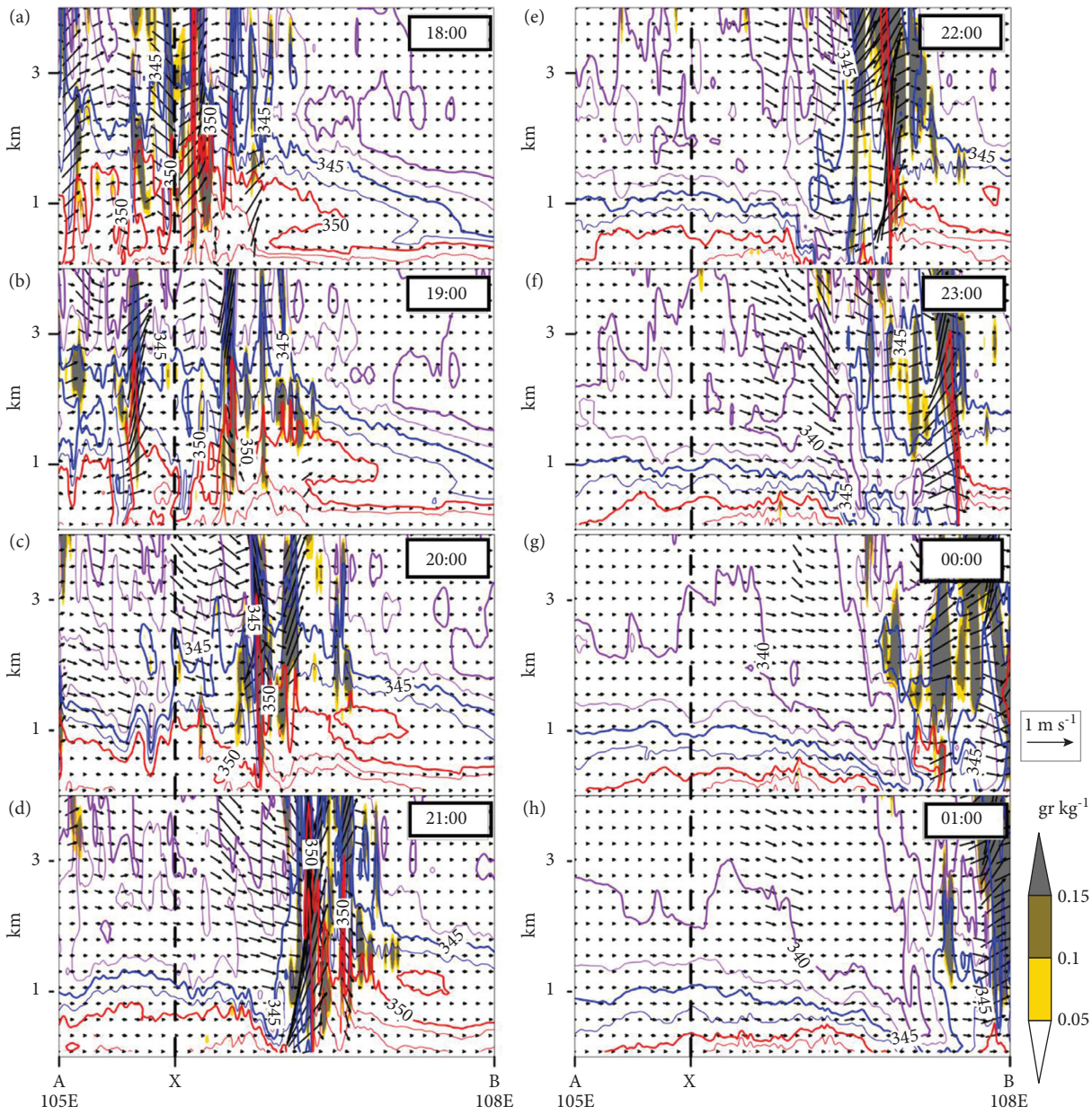

FIGURE 8: Vertical-longitude cross section of wind (vector; zonal component multiplied by a factor of 0.01), equivalent potential temperature (contour), and cloud mixing ratio (shaded) along the thick black line from point A to point B in Figure 6(b) with time evolution for (a-h) 18:00–01:00 LST. The x-axis is longitude representing the distance of A-B transect. The black vertical dotted line (X) indicated the coastal line. For clarity, the equivalent potential temperatures (θ_e) are differenced as contour lines with red for $\theta_e \geq 350$ K, blue for $350 > \theta_e \geq 345$ K, and purple for $345 > \theta_e \geq 340$ K. The purple contour line over near surface (<1 km) indicated a cold pool.

deep convective cells continuing was produced by the persistence of that CP until 02:00 LST over the middle sea. Thus, our model results indicate that CP propagation and advection by the north-westerly of background winds is a conceivable mechanism for the propagating convective systems due to the life cycle of MCC, which is consistent with the study by Li et al. [45] that mentioned that the direction of propagating diurnal rainfall is regulated by the prevailing background wind.

Hence, to calculate the speed phase of CP-coastal related to rainfall onset propagation and to investigate the offshore environment, time-height sections of CAPE, rainfall, and 0.5 km as well as 3 km temperature perturbation were chosen as further analyses (Figure 10). In this case, 3 km represents a depth of the maximum cool anomaly which has been reported in previous work [38]. In a rough estimation, the speed of CP-coastal is associated with rainfall onset propagation around $8.8\,\mathrm{m{\cdot}s^{-1}}$ (Figure 10(b)), which is in

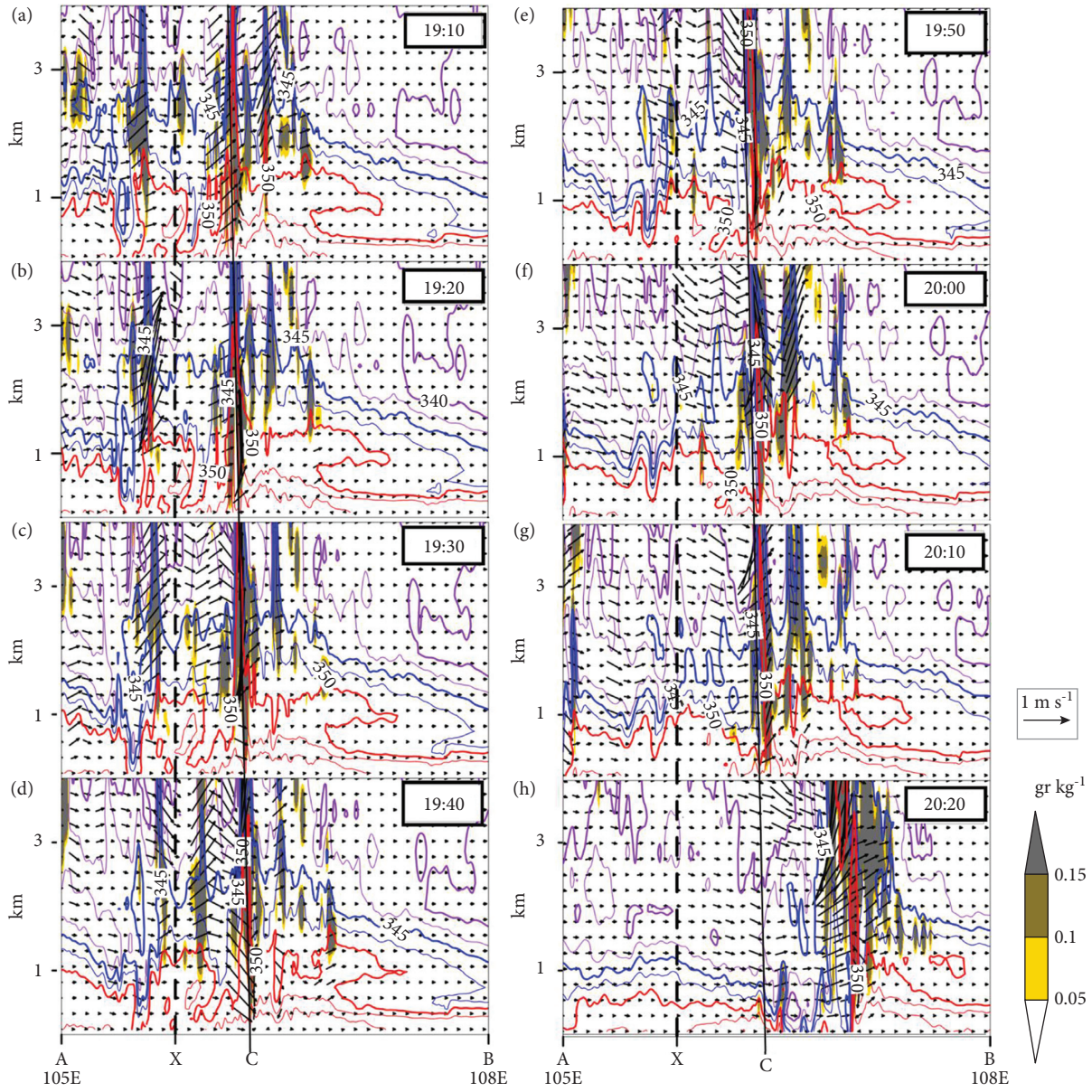

FIGURE 9: Same as Figure 8, but from 19:10 to 21:40 LST. The black vertical solid line (C) represents location (154 km from (X) of a stationary convection cell from 19:00 LST (see Figure 8) to 20:10 LST.

agreement with previous studies [46, 47]. This offshore rainfall propagation corresponds to a strong increase of CAPE (Figure 10(a)) as well as a cooling anomaly over the surface level at 0.5 km (Figure 10(c)). It appears that the offshore convective system was strongly maintained by the surface cold pool (CP-coastal) which moves offshore rapidly from late afternoon (18:00 LST) to early morning (02:00 LST). Interestingly, the initial convection around 16:00 LST over the seaside of the coastal region has strong connections with the land-based convective system under the consecutively CP-inland mechanism (Figure 10(d)). This was also shown by the existence of anomalies in a pair of warming and cooling as consecutively at low level (3 km) which is associated with developing a new convective cell from the previous decaying convection. This CP development is also triggering a deep convective cloud over the coastal region in the afternoon and maintaining a strong offshore propagation under the long-lasting MCC mechanism.

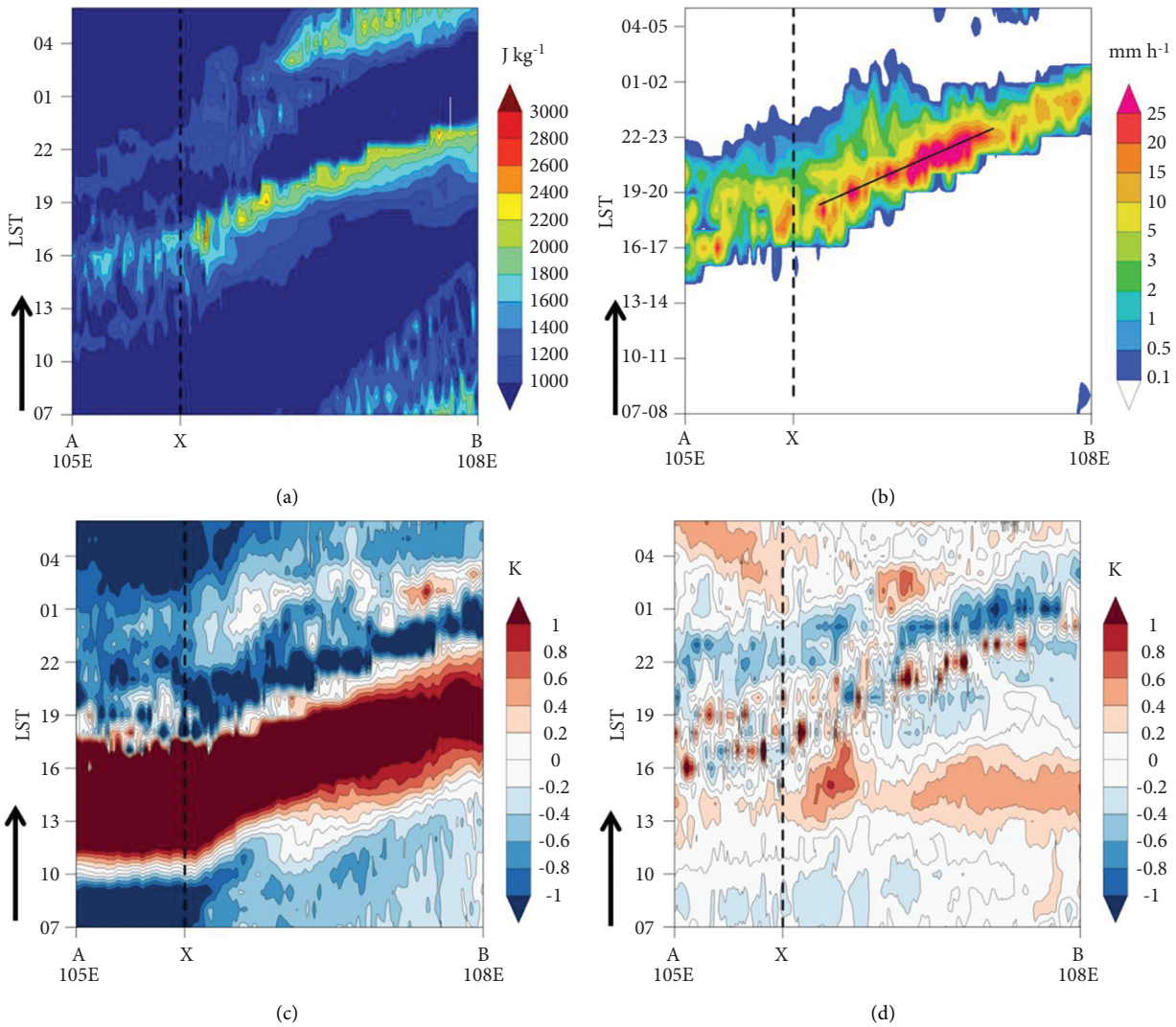

FIGURE 10: Diurnal cycle on January 1, 2021, for (a) CAPE, (b) rainfall, and temperature perturbations from daily mean, (c) 0.5 km, and (d) 3 km. Black dashed vertical lines indicate the position of the eastern coastline of South Sumatra. The phase speed of rainfall propagation of the red line is ~ 8.8 m·s^{-1}.

4. Conclusions

We have investigated the case study of a cold pool related to a heavy rainfall system during January 1-2, 2021, over Lampung, South Sumatra, by using the numerical weather prediction of the WRF model. Heavy rainfall observed by radar as well as satellite observations could be qualitatively well simulated by the model results. In this period, synoptic weather conditions due to the initial development of the Borneo vortex concurred to enhance the low-level north-westerly winds as a predominant prevailing wind over the wider area of Lampung, South Sumatra.

The development of CP related to offshore propagation of convective systems in this case study was illustrated by 2 categories: CP-inland and CP-coastal. The CP-inland propagates slowly and disappeared rapidly because of the relatively strong north-westerly wind due to the synoptic condition and lack of supporting environment related to near-surface moisture over the leading edge of the CP-inland. However, the dissipation of CP-inland strengthens the CP-coastal which is generated over the seaside of the coastal region. The CP-coastal tends to persist and propagates further offshore influenced by a large gradient between the near-surface equivalent temperature of CP and its environment. The CP-coastal which is developed as a result of decaying a deep convective cloud also induced the MCC by triggering new several convective clouds rapidly as well as spread under the back-building mechanism over the sea. Interestingly, the MCC developed in linear system which reported previously as mainly type of MCS over Java Sea (> 65%) occurred during January-February [47].

Moreover, it can be coarsely calculated from Figures 8 and 10 that the speed of the CP-coastal is around 8.8 m·s^{-1} (18:00–23:00 LST). This simulated CP speed is in agreement with the previous study [38] which founded that CP speed is 8 m·s^{-1} over the eastern Maritime Continent and [46] proposed that theoretically, the speed of CP is in a wide range around 5–12 m·s^{-1}. Additionally,

it was also found that the CP may have an important role to develop offshore-propagating convective systems which are influenced by prevailing background wind. Considering that the existence of the Borneo vortex during the southward monsoon flow period may have occurred [48] and coexist with Cross Equatorial Northerly Surge which is reinforcement by Cold Tongue [24], this heavy rainfall event could reoccur with varying intensity. We also noted that, for a heavy rainfall event, a WRF model with cloud permitting resolution of 1 km is able to capture small-scale processes related to the CP mechanism. For better prediction results improvement, we need more detailed monitoring data, correct analysis, and accurate short-range numerical weather prediction to anticipate and mitigate risk weather-related hydrometeorological disasters.

Data Availability

The datasets of NCEP-FNL, BMKG radar, Himawari satellite, GSMaP, CCMP, generated during and/or analysed in the current study are publicly available in the direct links: https://rda.ucar.edu/datasets/ds083.3/, http://www.bmkg.go.id/cuaca/citra-radar.bmkg/, http://weather.is.kochi-u.ac.jp/, ftp://rainmap:Niskur+1404@hokusai.eorc.jaxa.jp/, https://climatedataguide.ucar.edu/climate-data/ccmp-cross-calibrated-multi-platform-wind-vector-analysis.

Conflicts of Interest

The authors declare that there are no conflicts of interest regarding the publication of this paper.

Authors' Contributions

The author Erma Yulihastin is the main contributor to this manuscript who drafted the initial manuscript and revised it and improved discussions and the overall content of the manuscript. Ibnu Fathrio simulated the model and contributed to the significant findings. Trismidianto, Fadli Nauval, Wendi Harjupa, Elfira Saufina, and Danang Eko Nuryanto contributed to the production of related figures to validate the model. Didi Satiadi provided an additional claim in the introduction section. All the authors were involved in discussions during the review process and read and approved the final manuscript.

Acknowledgments

The authors would also like to express their appreciation to Dr. Tri Wahyu Hadi of Institut Teknologi Bandung for his useful discussions. The authors also greatly acknowledge BMKG for supporting station as well as radar data observations. This research supports the International Program of Years of the Maritime Continent (YMC) of 2017-2021 under the TerraMarris Research Collaboration. This research was supported by the Indonesia Educational Endowment Fund (LPDP) through the Mandatory Productive Innovative Research Program under National Research Priority (252/Menteri Ristek/Ka BRIN/E1/PRN/2020).

References

[1] H. R. Byers and R. R. Braham, *The Thunderstorm*, p. 287, U. S. Government Printing Office, Washington, DC, USA, 1949.
[2] J. Charba, "Application of gravity current model to analysis of squall-line gust front," *Monthly Weather Review*, vol. 102, no. 2, pp. 140–156, 1974.
[3] J. F. W. Purdom, "Some uses of high-resolution goes imagery in the mesoscale forecasting of convection and its behavior," *Monthly Weather Review*, vol. 104, no. 12, pp. 1474–1483, 1976.
[4] J. W. Wilson and W. E. Schreiber, "Initiation of convective storms at radar-observed boundary-layer convergence lines," *Monthly Weather Review*, vol. 114, no. 12, pp. 2516–2536, 1986.
[5] A. M. Tompkins, "Organization of tropical convection in low vertical wind shears: the role of cold pools," *Journal of the Atmospheric Sciences*, vol. 58, no. 13, pp. 1650–1672, 2001.
[6] G. Torri, Z. Kuang, and Y. Tian, "Mechanisms for convection triggering by cold pools," *Geophysical Research Letters*, vol. 42, no. 6, pp. 1943–1950, 2015.
[7] P. Gentine, A. Garelli, S. B. Park, J. Nie, G. Torri, and Z. Kuang, "Role of surface heat fluxes underneath cold pools," *Geophysical Research Letters*, vol. 43, no. 2, pp. 874–883, 2016.
[8] L. D. Grant and S. C. Heever, "Cold pool dissipation," *Journal of Geophysical Research: Atmosphere*, vol. 121, no. 3, pp. 1138–1155, 2016.
[9] A. J. Thorpe, M. J. Miller, and M. W. Moncrieff, "Two-dimensional convection in non-constant shear: a model of mid-latitude squall Lines," *Quarterly Journal of the Royal Meteorological Society*, vol. 108, no. 458, pp. 739–762, 1982.
[10] R. Rotunno, J. B. Klemp, and M. L. Weisman, "A theory for strong, long-lived squall lines," *Journal of the Atmospheric Sciences*, vol. 45, no. 3, pp. 463–485, 1988.
[11] K. K. Szeto and H.-R. Cho, "A numerical investigation of squall lines. Part III: sensitivity to precipitation processes and the coriolis force," *Journal of the Atmospheric Sciences*, vol. 51, no. 11, pp. 1341–1351, 1994.
[12] M. L. Weisman and R. Rotunno, ""A theory for strong long-lived squall lines" revisited," *Journal of the Atmospheric Sciences*, vol. 61, no. 4, pp. 361–382, 2004.
[13] R. M. Wakimoto, H. V. Murphey, C. A. Davis, and N. T. Atkins, "High winds generated by bow echoes. part II: the relationship between the mesovortices and damaging straight-line winds," *Monthly Weather Review*, vol. 134, no. 10, pp. 2813–2829, 2006.
[14] N. Jeevanjee and D. M. Romps, "Convective self-aggregation, cold pools, and domain size," *Geophysical Research Letters*, vol. 40, no. 5, pp. 994–998, 2013.
[15] R. Shi, Q. Cai, L. Dong, X. Guo, and D. Wang, "Response of the diurnal cycle of summer rainfall to large-scale circulation and coastal upwelling at hainan, south China," *Journal of Geophysical Research: Atmosphere*, vol. 124, no. 7, pp. 3702–3725, 2019.
[16] T. Kilpatrick, S.-P. Xie, and T. Nasuno, "Diurnal convection-wind coupling in the bay of bengal," *Journal of Geophysical Research: Atmosphere*, vol. 122, no. 18, pp. 9705–9720, 2017.
[17] A. Ricchi, D. Bonaldo, G. Cioni, S. Carniel, and M. M. Miglietta, "Simulation of a flash-food event over the adriatic sea with a high-resolution atmosphere–ocean–wave coupled system," *Scientific Reports*, vol. 11, pp. 1–11, 2021.
[18] S. Mori, H. Jun-Ichi, Y. I. Tauhid et al., "Diurnal land-sea rainfall peak migration over sumatera island, Indonesian

maritime," *Monthly Weather Review*, vol. 132, no. 8, pp. 2021–2039, 2004.

[19] C.-K. Teo, T.-Y. Koh, J. Chun-Fung Lo, and B. Chandra Bhatt, "Principal component analysis of observed and modeled diurnal rainfall in the maritime continent, observed by TRMM satellite and intensive rawinsonde soundings," *Journal of Climate*, vol. 24, no. 17, pp. 4662–4675, 2011.

[20] Trismidianto, T. W. Hadi, S. Ishida et al., "Development processes of oceanic convective systems inducing the heavy rainfall over the western coast of Sumatra on 28 october 2007," *Solanus*, vol. 12, pp. 6–11, 2016.

[21] M. D. Yamanaka, S. Y. Ogino, and P. M. Wu, "Maritime continent coastlines controlling earth's climate," *Progress in Earth and Planetary Science*, vol. 5, pp. 1–28, 2018.

[22] S. Mori, J. I. Hamada, and M. Hattori, "Meridional march of diurnal rainfall over jakarta, Indonesia, observed with a c-band Doppler radar an overview of the harimau2010 campaign," *Progress in Earth and Planetary Science*, vol. 5, pp. 1–23, 2018.

[23] J. H. Ruppert and F. Zhang, "Diurnal forcing and phase locking of gravity waves in the Maritime Continent," *Journal of the Atmospheric Sciences*, vol. 76, no. 9, pp. 2815–2835, 2019.

[24] E. Yulihastin, T. Wahyu Hadi, N. Sari Ningsih, and M. Ridho Syahputra, "Early morning peaks in the diurnal cycle of precipitation over the northern coast of West Java and possible influencing factors," *Annales Geophysicae*, vol. 38, no. 1, pp. 231–242, 2020.

[25] K. Kikuchi and B. Wang, "Diurnal precipitation regimes in the global tropics," *Journal of Climate*, vol. 21, no. 11, pp. 2680–2696, 2008.

[26] Y. Li, N. C. Jourdain, A. S. Taschetto et al., "Resolution dependence of the simulated precipitation and diurnal cycle over the maritime continent," *Climate Dynamics*, vol. 48, no. 11-12, pp. 4009–4028, 2017.

[27] I. Siregar, "Banjir bandang putus akses jalan, 250 kk di Pringsewu terisolasi," 2020, https://lampung.inews.id/berita/banjir-bandang-putus-akses-jalan-250-kk-di-pringsewu-terisolasi.

[28] W. C. Skamarock, J. B. Klemp, and J. Dudhia, *A Description of the Advanced Research WRF Version 3*, NCAR, Boulder, CO, USA, 2008.

[29] T. Kubota, S. Shige, H. Hashizume et al., "Global precipitation map using satellite-borne microwave radiometers by the GSMaP project: production and validation," *IEEE Transactions on Geoscience and Remote Sensing*, vol. 45, no. 7, pp. 2259–2275, 2007.

[30] K. Bessho, K. Date, M. Hayashi et al., "An introduction to himawari-8/9— Japan's new-generation geostationary meteorological satellites," *Journal of the Meteorological Society of Japan*, vol. 94, no. 2, pp. 151–183, 2016.

[31] R. A. Maddox, "Meoscale convective complexes," *Bulletin of the American Meteorological Society*, vol. 61, no. 11, pp. 1374–1387, 1980.

[32] R. A. Houze, "Cloud dynamics," *International Geophysics*, Academic Press, vol. 144pp. 573–575, Cambridge, MA, USA, 2nd edition, 2014.

[33] L. Ricciardulli and National Center For Atmospheric Research Staff, *The Climate Data Guide: CCMP: Cross-Calibrated Multi-Platform Wind Vector Analysis*, National Oceanic and Atmospheric Administration, Washington, DC, USA, 2017.

[34] R. Atlas, R. N. Hoffman, J. Ardizzone et al., "A cross-calibrated, multiplatform ocean surface wind velocity product for meteorological and oceanographic applications," *Bulletin of the American Meteorological Society*, vol. 92, no. 2, pp. 157–174, 2011.

[35] R. M. Fonseca, T. Zhang, and K.-T. Yong, "Improved simulation of precipitation in the tropics using a modified BMJ scheme in the WRF modelfied BMJ scheme in the WRF model," *Geoscientific Model Development*, vol. 8, no. 9, pp. 2915–2928, 2015.

[36] NOAA/NWS/NCEP, *NCEP GDAS/FNL 0.25 Degree Global Tropospheric Analyses and Forecast Grids*, NCAR Computational and Information Systems Laboratory Research Data Archive, Boulder, CO, USA, 2015.

[37] E. Kalnay, M. Kanamitsu, R. Kistler et al., "The NCEP/NCAR 40-year reanalysis project," *Bulletin of the American Meteorological Society*, vol. 77, no. 3, pp. 437–471, 1996.

[38] M. E. E. Hassim, T. P. Lane, and W. W. Grabowski, "The diurnal cycle of rainfall over new Guinea in convection-permitting WRF simulations," *Atmospheric Chemistry and Physics*, vol. 16, no. 1, pp. 161–175, 2016.

[39] R. S. Schumacher and R. H. Johnson, "Organization and environmental properties of extreme-rain-producing mesoscale convective systems," *Monthly Weather Review*, vol. 133, no. 4, pp. 961–976, 2005.

[40] W. Xiaofang, C. Chunguang, C. Wenjun, and S. Yan, "Modes of mesoscale convective system organization during meiyu season over the Yangtze river basin," *Journal of Meteorological Research*, vol. 28, pp. 111–126, 2013.

[41] R. S. Schumacher and K. L. Rasmussen, "The formation, character and changing nature of mesoscale convective systems," *Nature Reviews Earth & Environment*, vol. 1, no. 6, pp. 300–314, 2020.

[42] A. G. Laing and J. Michael Fritsch, "The global population of mesoscale convective complexes," *Quarterly Journal of the Royal Meteorological Society*, vol. 123, no. 538, pp. 389–405, 1997.

[43] E.-S. Im and E. A. B. Eltahir, "Simulation of the diurnal variation of rainfall over the western maritime continent using a regional climate model," *Climate Dynamics*, vol. 51, no. 1-2, pp. 73–88, 2017.

[44] N. J. Trilaksono, S. Otsuka, S. Yoden, K. Saito, and S. Hayashi, "Dependence of model-simulated heavy rainfall on the horizontal resolution during the jakarta flood event in january-february 2007," *SOLA*, vol. 7, pp. 193–196, 2011.

[45] Z. Li, P. Zuidema, and P. Zhu, "Simulated convective invigoration processes at trade wind cumulus cold pool boundaries," *Journal of the Atmospheric Sciences*, vol. 71, no. 8, pp. 2823–2841, 2014.

[46] A. Hutson, C. Weiss, and G. Bryan, "Using the translation speed and vertical structure of gust fronts to infer buoyancy deficits within thunderstorm outflow," *Monthly Weather Review*, vol. 147, no. 10, pp. 3575–3594, 2019.

[47] D. E. Nuryanto, H. Pawitan, R. Hidayat, and E. Aldrian, "The occurrence of the typical mesoscale convective system with a flood-producing storm in the wet season over the Greater Jakarta area," *Dynamics of Atmospheres and Oceans*, vol. 96, p. 101246, 2021.

[48] C.-P. Chang, P. A. Harr, and H.-J. Chen, "Synoptic disturbances over the equatorial south China sea and western maritime continent during boreal winter," *Monthly Weather Review*, vol. 133, no. 3, pp. 489–503, 2005.